

THREE-DIMENSIONAL NMR SPECTROSCOPY

Ad Bax, National Institutes of Health, Bethesda, Maryland 20892

Nearly two decades ago, a few years after the introduction of Fourier transform NMR, Jeener¹ was the first to point out the possibility of generating two-dimensional (2D) NMR spectra. Since then, aided by the availability of increasingly powerful computers, stronger magnets, and improved designs of NMR spectrometers, 2D NMR has become widely used in thousands of laboratories across the world. Applications vary from studying nuclear bond distances in solids² to determination of solution protein structures³ and non-invasive imaging of cross sections of the human body.⁴ Information is derived from experiments that usually consist of a sequence of radiofrequency pulses, spaced by time delays. A very large number of such experimental schemes, often referred to as pulse sequences, have found their way into the scientific literature.

From a chemical viewpoint, the NMR spectrum contains a wealth of information about electronic shielding of individual nuclei. Moreover, dihedral angles can be derived from *J* couplings using the well known Karplus equations and the process known as cross relaxation provides access to measuring interproton distances. Although, in principle, all this information can be extracted using one-dimensional (1D) NMR experiments, in practice the spectra of many substances of interest are so complex that a complete analysis is impossible. This is particularly true for larger molecules such as proteins, DNA fragments, oligosaccharides, and complex macrolites. In 2D NMR experiments, much of the overlap present in 1D spectra can often be removed, permitting a detailed interpretation of the spectral features.

Attempts to apply NMR to problems of ever increasing complexity, however, can result in 2D NMR spectra that are also too crowded for straightforward analysis. This is particularly the case for proteins larger than about 10 kD. Recently, the 2D NMR technology has been taken one step further, spreading the spectral information into three orthogonal frequency dimensions.

CHEMTRACTS—ANALYTICAL AND PHYSICAL CHEMISTRY 1:215-222 (1989)

© 1989 Chemtracts

CCC 0889-7810/89/040215-08\$4.00

Notice: This material may be protected
by copyright law (Title 17 U.S. Code)

PRINCIPLES OF 2D AND 3D NMR

Although the principles of 2D NMR have been discussed in many places,⁵ they will be briefly repeated here before discussing the extension to a third dimension. A general 2D pulse scheme consists of a preparation period, an evolution period, a mixing period, and a detection period (Fig. 1). During the preparation period, magnetization returns to its equilibrium state, and at the end of the preparation period a single pulse or a combination of radio-frequency pulses creates a transient state of the spin system. This transient state then evolves for a variable time period, t_1 , and subsequently a set of pulses and delays (mixing period) is used to mix the coherence present during t_1 with signals from other nuclei that are then detected during the time t_2 . A tremendous number of different mixing schemes can be used, depending on the effect one wants to study. A 2D pulse scheme, such as schematically shown in Figure 1, is executed many times, with the duration of the evolution period, t_1 , systematically incremented (typically from 0 to about 100 ms, in steps of a few hundred μ s). The spectra, obtained for each of the t_1 durations are stored separately and without going into a detailed description, suffice it to say that the resonance intensities in the 1D spectra (obtained for every t_1 duration) are sinusoidally modulated as a function of t_1 . Fourier transformation of these modulation patterns, with respect to the time variable t_1 , converts this set of 1D spectra into a 2D spectrum (Fig. 2). In this spectrum, the two frequency coordinates, F_1 and F_2 , of a particular resonance correspond to the precession frequencies associated with the observed magnetization during t_1 and t_2 , respectively. For example, the resonance in Figure 2(C) at coordinates $(F_1, F_2) = (\Omega_A, \Omega_B)$ corresponds to that portion of the magnetization that originated on the protons of methyl group A which because of a 180° flip about the C—N bond during the mixing period precesses (resonates) with the frequency of methyl group B during the time t_2 .

As indicated above, the second frequency dimension in 2D NMR spectra originates from the Fourier transformation of the t_1 modulation patterns in the 1D spectra. Two 2D pulse schemes can be combined into a single 3D experiment by replacing the detection period of the first 2D experiment by the evolution period of the second 2D experiment (Fig. 1). The detection period is now relabeled " t_3 ," and for every duration of the new time variable, t_3 , a complete (t_1, t_2) 2D data set is acquired. The intensities of the resonances in the 2D spectra are modulated as a function of the new time variable, t_3 . Fourier transformation of t_3 sections taken through these 2D data sets converts the set of 2D spectra into a 3D NMR spectrum, where the frequency coordinates, F_1 , F_2 , and F_3 correspond to the correlated resonance frequencies present during the times t_1 , t_2 , and t_3 . This procedure will be illustrated for the conceptually simplest case of heteronuclear 3D NMR. The 3D pulse

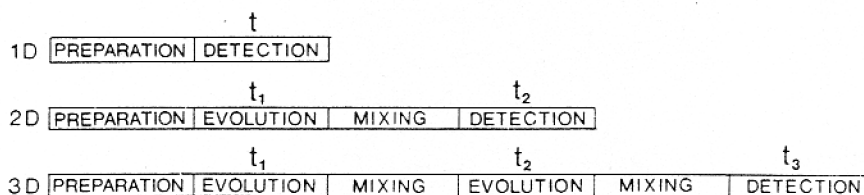


Figure 1. Schematic representation of one-, two-, and three-dimensional NMR experiments.

Fig. 2.
for a s
A Fou
showr
from S

many places.
sion to a third
ion period, an
fig. 1). During
m state, and at
ation of radio-
This transient
uently a set of
present during
g the time t_2 . A
i, depending on
is schematically
of the evolution
bout 100 ms. in
the t_1 durations
ription, suffice it
ined for every t_1
Fourier transfor-
time variable t_1 .
In this spectrum,
rrence correspond
ed magnetization
in Figure 2(C) at
on of the magnet-
hich because of a
cesses (resonates)

2D NMR spectra
ilation patterns in
into a single 3D
2D experiment by
1). The detection
new time variable.
s of the resonances
v time variable. t_2
2D data sets convert
ne frequency coordi-
onance frequencies
ll be illustrated for
AR. The 3D puls

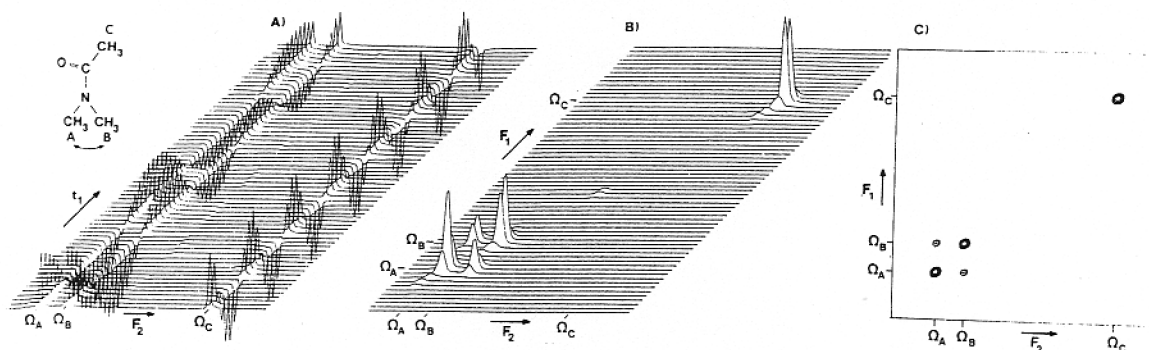


Fig. 2. The generation of a 2D exchange spectrum of *N,N*-dimethylacetamide. (A) A set of 1D spectra obtained for a series of t_1 durations. The resonance frequencies of methyl groups A, B, and C are labeled Ω_A , Ω_B , and Ω_C . A Fourier transformation with respect to t_1 of the columns of the matrix of data set (A) yields the 2D spectrum shown in (B). For clarity, such a spectrum is commonly displayed as a contour plot (C). Reprinted with permission from *Science*. © 1986 AAAS.

scheme [Fig. 3(c)] combines the 2D NOESY pulse scheme⁶ [Fig. 3(a)] with a heteronuclear shift correlation experiment first proposed by Bodenhausen and Ruben⁷ [Fig. 3(b)].

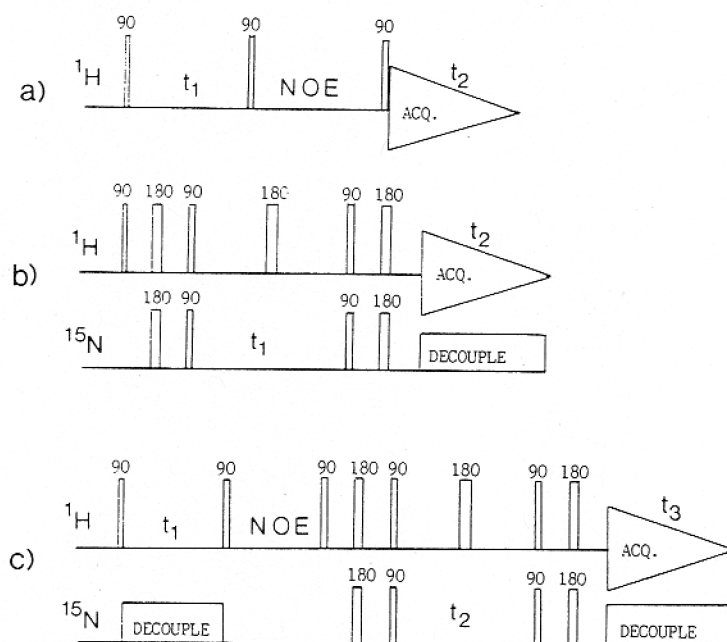


Figure 3. Pulse schemes of the (a) the 2D NOESY experiment, (b) the 2D ^1H -detected Overboderhausen experiment, and (c) the NOESY-Overboderhausen 3D sequence. The NOESY spectrum yields off-diagonal resonances for pairs of protons that are close in space, with intensities that depend, to first order, on the inverse sixth power of the interproton distances. The Overboderhausen experiment yields high sensitivity spectra where the resonance coordinates correspond to the proton chemical shift (F_2) and the chemical shift of the heteronucleus (^{15}N or ^{13}C) along the F_1 axis.

Consider first the case where the new time variable in Figure 3(c), t_2 , is kept constant (zero). By incrementing the t_1 time variable, a 2D NOESY spectrum is obtained, similar to what would be obtained with the NOESY scheme of Figure 3(a). In the mixing period of the NOESY experiment, spatially proximate protons exchange their nuclear magnetization at rates proportional to r^{-6} , where r is the interproton distance. Off-diagonal resonance (cross peak) intensities in such a NOESY spectrum are therefore a measure for interproton distance. In protein spectra, many of the NOE cross peaks overlap and identification may become impossible. 3D NMR attacks this problem by introducing a third time variable into the sequence. Thus, the center part of the 3D pulse scheme transfers the transverse ^1H magnetization to its directly attached heteroatom (either ^{15}N or ^{13}C), where it then resonates at the ^{15}N or ^{13}C frequency for a time period t_2 , and subsequently it is transferred back to the ^1H nucleus. Its magnetization is observed during the time t_3 . The time variable t_2 is incremented for successive experiments. The amount of back transfer to the ^1H is sinusoidally modulated (as a function of t_2) by the ^{15}N or ^{13}C frequency. For practical reasons, in a single experiment one can only transfer to one type of heteronucleus, either ^{13}C or ^{15}N , and for sensitivity reasons, isotopic enrichment is often essential. After Fourier transformation with respect to the time variables t_1 and t_3 , a set of 2D spectra is obtained where the intensities are t_2 -modulated by the chemical shift of the heteronucleus that is directly attached to the proton observed during t_3 . A set of such 2D spectra is drawn in Figure 4(a). Fourier transformation in the t_2 dimension transforms this set of 2D spectra into the final 3D spectrum. Note that the t_2 Fourier transformation transforms the signals that are spread over the entire ensemble of t_2 planes into single peaks in the 3D spectrum, greatly increasing the intensity. Because the noise remains evenly distributed throughout the 3D spectrum, the signal-to-noise ratio in the 3D spectrum is much

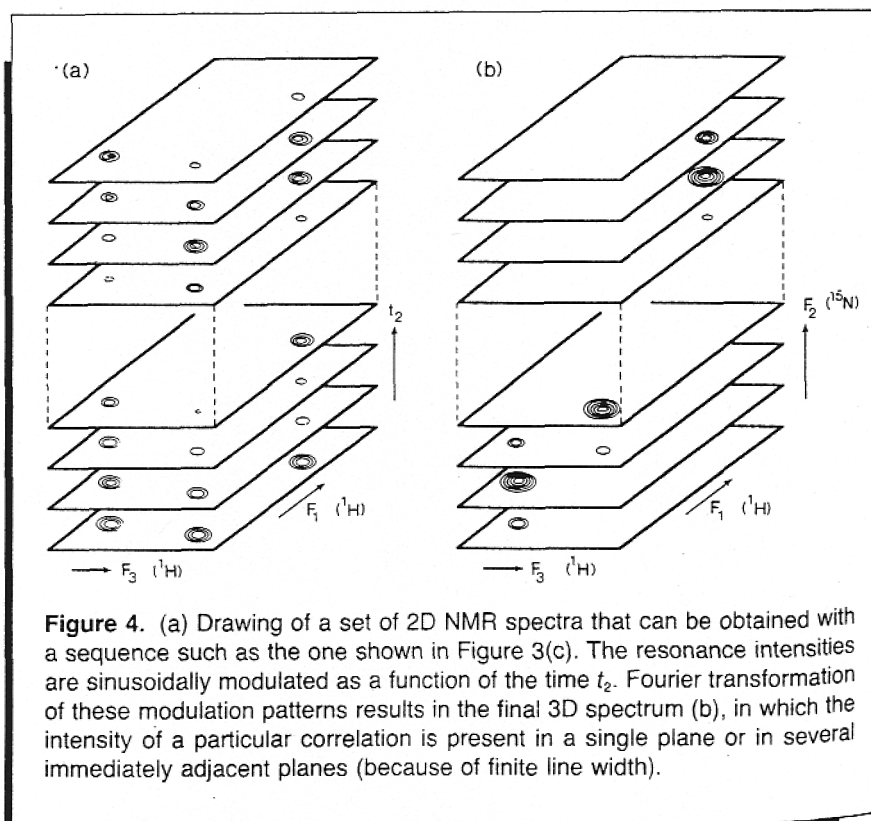
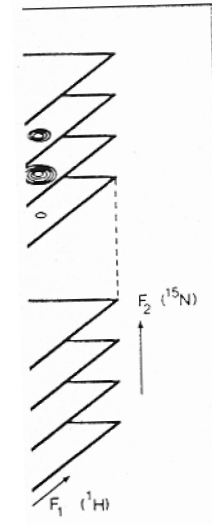


Fig
the
of
am

re 3(c), t_2 , is kept
 NOESY spectrum
 OESY scheme of
 nt, spatially prox-
 es proportional to
 ance (cross peak)
 re for interproton
 overlap and iden-
 problem by intro-
 center part of the
 on to its directly
 onates at the ^{15}N
 ; transferred back
 time t_3 . The time
 ; amount of back
 of t_2 by the ^{15}N
 rent one can only
 ind for sensitivity
 er transformation
 ectra is obtained
 ift of the hetero-
 uring t_3 . A set of
 rmation in the t_2
 O spectrum. Note
 it are spread over
 spectrum, greatly
 istributed through-
 spectrum is much



be obtained with
 ance intensities
 r transformation
 (b), in which the
 re or in several

higher than in the individual t_2 slices. Display of the 3D spectrum can be accomplished by adapting software originally developed for molecular graphics. However, more commonly, slices taken from the 3D spectrum are displayed as regular 2D contour maps.

As an example, Figure 5 shows a (F_1, F_3) slice from the NOESY-HMQC 3D spectrum of the protein staphylococcal nuclease (18 kD) and compares it with the corresponding region of the regular 2D NOESY map. The 3D spectrum has been recorded with a method very similar to the one shown in Figure 3(c), and separates NOE interactions involving amide protons according to the chemical shift of the ^{15}N nucleus that is directly attached to the amide proton that is detected during the time t_3 . The entire 3D spectrum consists of 64 such slices. Clearly, the almost complete absence of resonance overlap in the 3D example greatly facilitates the analysis of such a spectrum.

The heteronuclear 3D NMR experiments are extremely powerful because (a) they are very sensitive (provided that isotopic enrichment is used) and (b) because their interpretation is very straightforward.⁷⁻¹⁰ The high sensitivity results from the fact that the heteronuclear magnetization transfer occurs via relatively large one-bond J couplings, providing nearly 100% efficiency. A second factor that aids the sensitivity of the 3D method is that often some line broadening digital filtering must be used to avoid truncation artifacts.

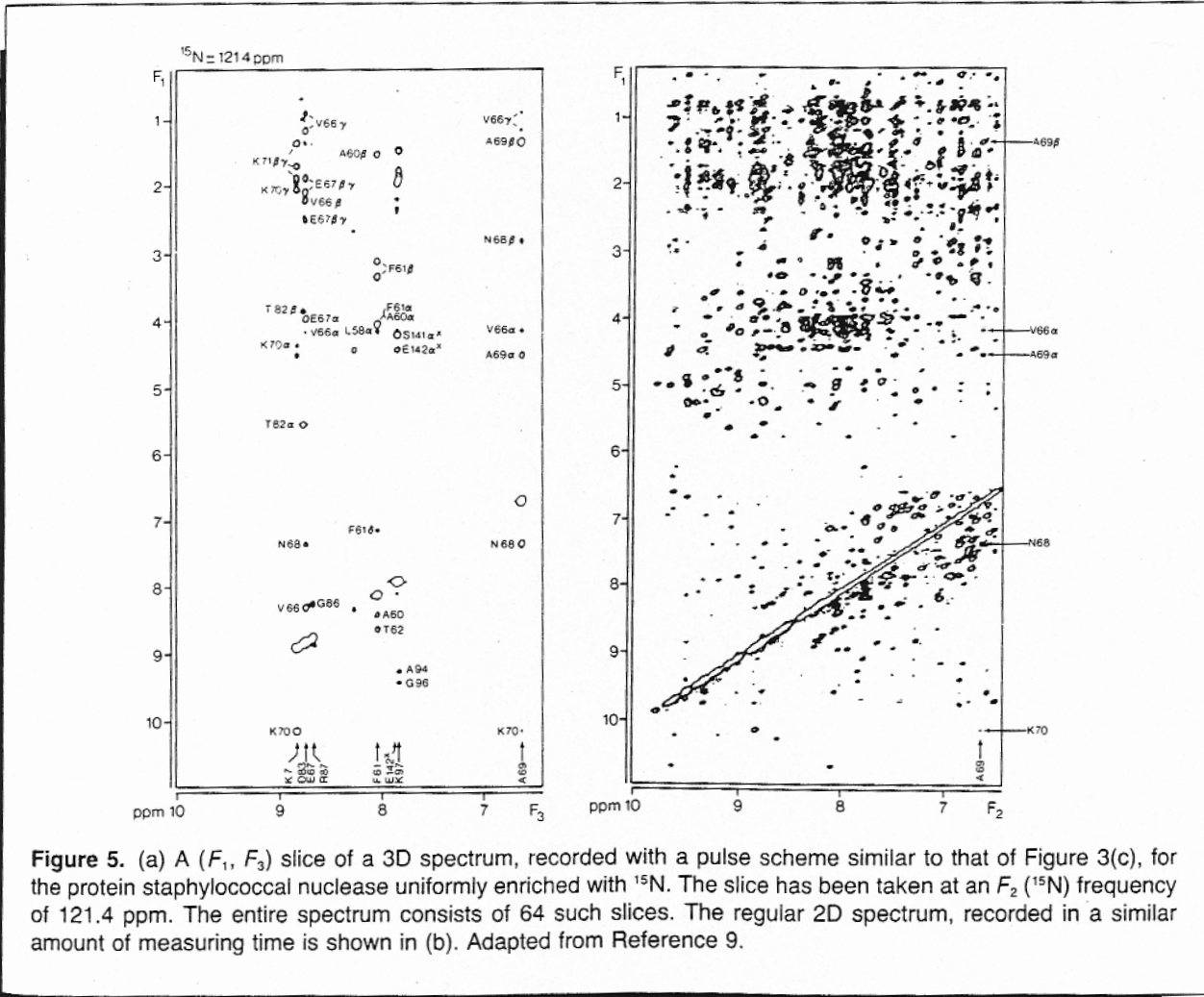


Figure 5. (a) A (F_1, F_3) slice of a 3D spectrum, recorded with a pulse scheme similar to that of Figure 3(c), for the protein staphylococcal nuclease uniformly enriched with ^{15}N . The slice has been taken at an F_2 (^{15}N) frequency of 121.4 ppm. The entire spectrum consists of 64 such slices. The regular 2D spectrum, recorded in a similar amount of measuring time is shown in (b). Adapted from Reference 9.

This slightly increases the signal-to-noise ratio of the spectrum. In contrast, strong resolution enhancement is often required for 2D spectra in order to reduce spectral overlap, decreasing the signal-to-noise ratio.

For many structural problems of interest, isotopic enrichment may be very difficult or impossible. However, for smaller soluble substances the heteronuclear 3D NMR experiment can also be conducted at natural abundance.¹² Of course, when using natural abundance ^{13}C , the sensitivity of the 3D experiment is about two orders of magnitude lower relative to the comparable 2D ^1H - ^1H experiment. Because homonuclear ^1H - ^1H J couplings are often at least partially resolved for these smaller substances, homonuclear 3D experiments are also feasible. The first 3D NMR experiments proposed^{13,14} were of the purely homonuclear ^1H type. The projection on the (F_1, F_3) plane of such a 3D spectrum shows a regular J correlation (COSY) spectrum.¹⁵ In the other dimension (F_2), the J coupling multiplet pattern is present. The main reason why this particular 3D experiment was attempted first is the fact that the spectral width in the added dimension (F_2) can be very narrow (<50 Hz), enabling good digital resolution with a relatively small 3D data matrix (with as little as 16 F_2 planes). More powerful homonuclear ^1H 3D experiments were proposed subsequently,¹⁵⁻¹⁷ combining popular 2D pulse schemes such as NOESY and an experiment known as TOCSY¹⁸ or HOHAHA¹⁹ or even NOESY and NOESY. Recently, Griesinger et al.²⁰ presented a systematic overview of the different possible combinations of 2D NMR experiments that result in potentially useful 3D experiments, including a detailed analysis of 3D line shapes and sensitivity.

As a last example, Figure 6 shows the 3D NOESY-HOHAHA spectrum of the protein pike parvalbumin. According to Vuister et al.¹⁶ the spectrum

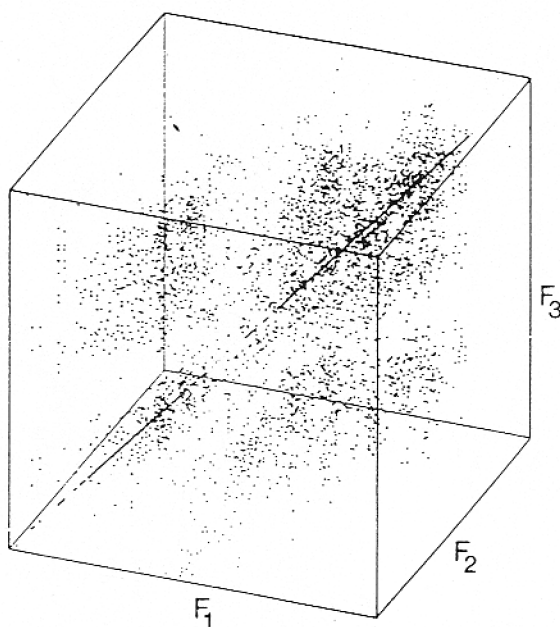


Figure 6. 3D NOE-HOHAHA spectrum of the protein parvalbumin. Reprinted with permission from the *Journal of Magnetic Resonance*. © 1988 Academic Press.

contains over 50,000 peaks. Recording this spectrum required about one week of measuring time. However, analysis of all the information present takes much longer. In this particular spectrum, a resonance at frequency coordinates $(F_1, F_2, F_3) = (\delta_A, \delta_B, \delta_C)$ corresponds to magnetization that is transferred via the NOE effect from proton A to proton B and subsequently, during the HOHAHA mixing period to proton C, where δ is the chemical shift frequency. Because two relatively inefficient transfer steps (NOE and HOHAHA) are involved, the sensitivity of the informative double-transfer cross peaks is low. However, in contrast to the heteronuclear 3D experiment, this type of methodology provides new information not present in a single 2D spectrum. This technique is particularly powerful in defining from the same data set both the through-bond and through-space connectivities, immediately identifying, for example, intra-residue NOE interactions. In contrast, with 2D spectroscopy separate experiments must be performed to obtain both J connectivity and NOE information. Moreover, resonance overlap present in the 2D spectra is again largely removed in the 3D spectrum.

The 3D methods described above are logical extensions of the concepts developed for 2D NMR spectroscopy. It is clear that a 3D spectrum provides the spectral information in the most resolved form. In fact, 2D spectra can always be considered as projections of a 3D spectrum, whereby the frequency encoding along the projection axis has disappeared. The main practical problems of 3D NMR are the large size of the 3D data matrix typically required and the long measuring time. The measuring time for 3D experiments is dictated by the number of t_1 and t_2 increments that are needed to obtain sufficient resolution in the F_1 and F_2 dimensions. For example, using modest numbers of 256 increments in both the t_1 and t_2 dimensions, this requires the pulse sequence to be repeated at least 256×256 times. Quite often, for each (t_1, t_2) pair the pulse sequence has to be repeated a number of times with different phases of the rf pulses to select a desired coherence transfer pathway²¹ in a process known as phase cycling. A very short four-step phase cycle brings the total number of repetitions of the pulse sequence then up to 262144. Assuming every individual execution of the pulse sequence takes 1.5 s, the total measuring time is 4.5 days. Of course, this makes routine recording of 3D spectra difficult, and it is therefore expected that this type of methodology, although extremely powerful, will remain restricted to the applications where it is most needed, i.e., the study of biological macromolecules.

REFERENCES

1. Jeener, J. Ampere International Summer School, Basko Polje, Yugoslavia, 1971, unpublished lecture.
2. Rybaczewski, E.F., Neff, B.L., Waugh, J.S., Sherfinski, J.S. *J. Chem. Phys.* **1977**, 67, 1231; Munowitz, M.G., Aue, W.P., Griffin, R.G. *J. Chem. Phys.* **1982**, 77, 1686.
3. Wuthrich, K. *NMR of Proteins and Nucleic Acids*, Wiley: New York, 1986; Clore, G.M., Gronenborn, A.M. *CRC Critical Reviews* **1989**, 24, in press; Bax, A. *Ann. Rev. Biochem.* **1989**, 58, 223.
4. Young, S.W. *Nuclear Magnetic Resonance Imaging: Basic Principles*, Raven Press: New York, 1984.
5. Bax, A. *Two-Dimensional Nuclear Magnetic Resonance*, Reidel: Boston, 1982.; Ernst, R.R., Bodenhausen, G., Wokaun, A. *Principles of Nuclear Magnetic Resonance in One and Two Dimensions*, Clarendon Press: Oxford, 1987.; Kessler, H., Gehrke, M., Griesinger, C. *Angew. Chem. Int. Ed. Engl.* **1988**, 27, 490.

6. Jeener, J., Meier, B.H., Bachmann, P., Ernst, R.R. *J. Chem. Phys.* **1979**, 71, 4546.; Macura, S., Ernst, R.R. *Mol. Phys.* **1980**, 41, 95.
7. Bodenhausen, G., Ruben, D.J. *Chem. Phys. Lett.* **1980**, 69, 185.
8. Fesik, S.W., Zuiderweg, E.R.P. *J. Magn. Reson.* **1988**, 78, 588.
9. Marion, D., Kay, L.E., Sparks, S.W., Torchia, D.A., Bax, A. *J. Am. Chem. Soc.* **1989**, 111, 1515.
10. Zuiderweg, E.R.P., Fesik, S.W. *Biochemistry* **1989**, 28, 2387.
11. Marion, D., Driscoll, P.C., Kay, L.E., Wingfield, P.T., Bax, A., Gronenborn, A.M., Clore, G.M. *Biochemistry* **1989**, 28, 6150.
12. Fesik, S.W., Gampe, R.T., Zuiderweg, E.R.P. *J. Am. Chem. Soc.* **1989**, 111, 770.
13. Plant, H.D., Mareci, T.H., Cockman, M.D., Brey, W.S. 27th ENC Conference, Poster A23, Baltimore, MD, 1986.
14. Vuister, G.W., Boelens, R. *J. Magn. Reson.* **1987**, 73, 328.
15. Oschkinat, H., Griesinger, C., Kraulis, P.J., Sorensen, O.W., Ernst, R.R., Gronenborn, A.M., Clore, G.M. *Nature (London)* **1988**, 332, 374; Oschkinat, H., Ciesler, C., Gronenborn, A.M., Clore, G.M. *J. Magn. Reson.* **1989**, 81, 212.; Oschkinat, H., Ciesler, C., Holak, T.A., Gronenborn, A.M., Clore, G.M. *J. Magn. Reson.* **1989**, 83, 450.
16. Vuister, G.W., Boelens, R., Kaptein, R. *J. Magn. Reson.* **1988**, 80, 176.
17. Boelens, R., Vuister, G.W., Koning, T.M.G., Kaptein, R. *J. Am. Chem. Soc.*, in press.
18. Braunschweiler, L., Ernst, R.R. *J. Magn. Reson.* **1983**, 53, 521.
19. Bax, A., Davis, D.G. *J. Magn. Reson.* **1985**, 65, 355.
20. Griesinger, C., Sorensen, O.W., Ernst, R.R. *J. Magn. Reson.* **1989**, 84, 14.
21. Bodenhausen, G., Kogler, H., Ernst, R.R. *J. Magn. Reson.* **1984**, 58, 370.

PURPOS

WHAT F
ACCOM

RESEA